H-Mat Hydrogen Compatibility of NBR Elastomers

Simmons, K.L.[1], Kuang, W.[1], Dohnalkova, A.[1], Arey, B.W.[1], Shin, Y.[1], and Menon, N.C.[2]

[1] Pacific Northwest National Laboratory, PO Box 999, Richland, WA 99354, USA, kl.simmons@pnnl.gov
[2] Sandia National Laboratories, 7011 East Avenue, Livermore, CA 95391, USA, ncmenon@sandia.gov

ABSTRACT
The H2@Scale program of the U.S. Department of Energy (DOE) Hydrogen and Fuel Cell Technologies Office (HFTO) is supporting work on the hydrogen compatibility of polymers to improve the durability and reliability of materials for hydrogen infrastructure. The hydrogen compatibility program (H-Mat) seeks "to address the challenges of hydrogen degradation by elucidating the mechanisms of hydrogen-materials interactions with the goal of providing science-based strategies to design materials, (micro)structures, and morphology with improved resistance to hydrogen degradation." Previous work on ethylene propylene diene indicated hydrogen interaction with plasticizer increased its migration to the surface and coalescing within the elastomer compound. New research on nitrile butadiene (NBR) has found hydrogen and pressure interactions with a series model rubber-material compounds to behave similarly in some compounds and improved in other compounds that is demonstrated through volume change and compression-set differences in the materials. Further studies were conducted using a helium-ion microscope (HeIM), which revealed significant morphological changes in the plasticizer-incorporating compounds after static exposure and pressure cycling, as evidenced by time-of-flight secondary ion mass spectrometry. Additional studies using x-ray chromatography revealed that more micro-voids/-cracks developed after gas decompression in unfilled materials than in filled materials; transmission electron microscopy (TEM) probed at the nano-meter level showing change in filler distribution and morphology around Zinc-based particles.

1.0 INTRODUCTION

The global energy sector views clean energy carriers as a viable solution to reduce dependence on fossil fuels for both mobile applications and stationary power supplies. [1,2] Hydrogen has gained increased visibility due to its high energy density which is almost three times more than diesel or gasoline. The United States Department of Energy's Hydrogen and Fuel Cell Technologies Office (HFTO) has initiated an H2@Scale program to expand the use of hydrogen as another energy carrier to support the electrical infrastructure and industry. However, the broad use of hydrogen is currently constrained by its potential incompatibility with materials when they are exposed for long periods of time at high pressure.[3,4] Looking forward to address material challenges in hydrogen related applications, the hydrogen materials compatibility program (H-Mat) is situated for cross-cutting basic science research and development on hydrogen materials compatibility, co-led by Pacific Northwest National Laboratory (PNNL) and Sandia National Laboratories (SNL). H-Mat research & development (R&D) activities cover both metals and polymers of interest, both computationally and experimentally, in the hydrogen infrastructure and onboard applications. In this program, efforts have been taken to (1) develop models of hydrogen transport and hydrogen-induced degradation of polymers at multiple length scales to inform materials evaluation and design, (2) quantify the relationship between hydrogen pressure-temperature-time-damage and polymers, (3) discover modified and new materials systems with greater resistance to hydrogen, (4) quantify hydrogen effects at microstructural length scales in select metals, (5) quantify damage and crack nucleation in select metals in hydrogen environments, (6) evaluate composite materials, select metals, and weld materials in cryogenic conditions, and other topics. (More information can be found at DOE H-Mat website) PNNL is leading the research activities regarding polymers, to test the effects of high pressure hydrogen on materials performance associated with current hydrogen energy technologies in delivery and distribution, fueling stations, and transportation fueling systems. Specifically, high-pressure hydrogen has been found various metals to undergo embrittlement and structural damage. [5-8] Unlike metals, the hydrogen community commonly considered polymers chemically inert to hydrogen as research shows that any damage primarily results from mechanical failure which primarily occurs during sudden decompression of high-pressure hydrogen. This type of damage is commonly referred to as explosive decompression failure (XDF) [9,10]; it has been investigated in several studies due to growing interest in high-pressure hydrogen applications. Mechanistically, the hydrogen absorbed within the polymer matrix undergoes sudden expansion during the rapid removal of external pressure, which engenders bubbles, surface blistering, material extrusion, or even catastrophic failure by exfoliation.

Yamabe *et al.* [11] conducted blister tests and hydrogen content measurements for ethylene-propylene rubber (EPDM) and nitrile-butadiene rubber (NBR) containing carbon black, silica, and no fillers after exposure to hydrogen at 10 MPa. They found that carbon black raises the hydrogen content of the material while silica mitigates blister damage. They also investigated the decompression-induced blister damages and the change in permeability of rubber O-rings as a function of hydrogen pressure and temperature [12]. Later on, they exposed the rubber O-rings to hydrogen at 100 MPa and performed fracture analysis based on the non-linear finite element modeling [13]. In 2011, Yamabe *et al.* [14] came up with an acoustic emission method to detect internal fracture of rubber seals caused by rapid decompression of 0.7 MPa hydrogen gas, and correlated the acoustic emission signals with the increase in number and size of internal cracks. Atomic force microscopy (AFM) was adapted to explore the relationship between decompression-induced internal fracture and microstructure of EPDM, revealing two fracture processes: bubble formation at a sub-micrometer level and crack initiation at a micrometer level [15]. Furthermore, Fujiwara *et al.* [16] first reported on characterizing the dissolved hydrogen in rubber materials with nuclear magnetic resonance (NMR) and established an advanced method to quantitatively estimate the dissolved hydrogen based on peak area of the characteristic peaks [17]. Solid-state NMR and liquid-phase NMR were utilized by Fujiwara *et al.* [18] to evaluate the possible change in chemical structure of NBR exposed to high-pressure hydrogen at 100 MPa. The results suggested no chemical changes occurred to NBR and the cause of XDF was likely to be mechanically dissolved hydrogen. Koga *et al.* [19] employed a high-pressure durability tester where rubber O-rings are pressure cycled in high-pressure hydrogen environments, suggesting that the material, temperature, O-ring filling ratio, and decompression time are sensitive factors among others.

Yamabe *et al.* [20] elaborated on the effects of no fillers, carbon black and silica on the volumetric expansion, hydrogen content, and tensile properties of sulfur-cured NBR in the hydrogen pressure range of 0.7-100 MPa. Along this line, they molded O-rings from a filled, peroxide-cured EPDM for cyclic exposure to hydrogen with pressures ranging from 10 to 70 MPa and temperatures ranging from 30 to 100 °C [21]. Their finding indicated that cracks (blisters) were caused by bubbles formed from supersaturated hydrogen molecules after decompression. More recently, the hydrogen degradation of NBR unfilled and filled with carbon black or silica was examined from the mechanical perspective [22]. Neither hydrogenation nor chain scission was found according to the corresponding NMR spectra, consistent with their prior work. Deterioration of the filler-gel structure form at the interface of the filler and polymer was attributed to the reduced elastic modulus after cyclic high-pressure hydrogen exposure. Fujiwara [23] reported on the effects of carbon black type and crosslinking density on impregnated hydrogen content and volume change as well as the effects of silica coupling agent for NBR. In 2018, Ohyama *et al.* [23] leveraged small-angle X-ray scattering in understanding the early stage of XDF failure of NBR released from high-pressure hydrogen environments and concluded that the inhomogeneity of the crosslink density resulted in the low-density phase within the material where there is a high possibility for larger voids to form. Castagnet *et al.* [24] created an X-ray computed tomography-based approach of producing 3D imaging of decompression failure in high-pressure hydrogen exposed EPDM, offering rigorous estimation of volume distribution of cavities. Jung *et al.* [25] demonstrated the use of nondestructive impedance spectroscopy for an in-situ quantification of hydrogen penetration into and hydrogen desorption out of NBR, supported by a COMSOL simulation based on their scanning electron microscopy observations.

Most recently, Kim *et al.* [26] dived into the effects of various particle size of carbon black on the physical properties (e.g., volume change, hardness, tensile properties, etc.) of EPDM exposed to hydrogen of 87.5 MPa for 168 hours. They pointed out that smaller particle size of carbon black leads to a higher level of resistance to hydrogen degradation. Jung *et al.* [27] exhibited three techniques for measuring the transport properties of a group of rubbers, gas chromatography by thermal desorption analysis, volumetric collection measurement of hydrogen by graduated cylinder and gravimetric measurement by electronic balance, finding no significant pressure dependence for hydrogen diffusivity and permeability. In our own research, we investigated a series of model NBR materials and discovered the phase separation of an oil-based plasticizer (dioctyl sebacate) in NBR which is driven by the change in solubility due to hydrogen exposure [28]. We also evaluated the tribological performance of model EPDM and NBR materials under both ambient and high-pressure hydrogen environments with our unique in-situ tribology testing capability [29].

In light of our prior work [28], the present work was focused on, to further our understanding in hydrogen-polymer interaction as well as potential damage mechanism when subject to high pressure hydrogen. NBR was selected as the model material for this work due to its good chemical resistance and gas barrier properties, making them favorable in many applications in fuel hoses, gaskets, O-rings, seals, and among others. The compression set of a material is oftentimes a huge consideration when selecting the best material for a gasket application as it measures the permanent deformation of the material remaining after the external force is removed, and usually is expressed as a percentage. As the rubber gasket is compressed over time or repeatedly, it loses the ability to revert to its original shape when the material has a high percentage (i.e., poor resistance to permanent deformation). Therefore, the sealing performance of the rubber gasket is reduced which may eventually cause a leak and component failure. Therefore, compression set and density change (inversely proportional to volume change) of the compounds were

first studied to examine effects of high-pressure hydrogen on the model materials from a macroscopic perspective. To achieve better performance for a specific application, commercially available rubber materials utilize additives such as fillers (e.g., silica, carbon black) for modifying and targeting specific properties such as hardness and plasticizer (e.g., DOS) for low temperature characteristic. However, the incorporation of these additives not only complicates the compounding in production but also creates interfaces with the rubber matrix which might be the origin of the hydrogen-induced damage people have seen in these materials. To visualize possible changes in structure/morphology of the model materials, PNNL's advanced characterization techniques such as HeIM, TEM, and time-of-flight secondary ion mass spectrometry (TOF-SIMS) were adopted to evaluate and comprehend the influences of high-pressure hydrogen at the molecular level.

2.0 MATERIALS AND METHODS

2.1 Model materials

A series of six NBR model compounds was developed for this research in collaboration with Kyushu University Fukuoka, Japan and Takaishi Industry Co., Ltd. Osaka, Japan. The work reported here focuses on four (4) NBR compounds, as specified in Table 1. The compound formulation NBR-nF-nP is a vulcanized NBR elastomer without any plasticizer or fillers. The compound formulation NBR-nF-P is a vulcanized NBR elastomer with a DOS plasticizer and no carbon black or silica filler. NBR compound NBR-F-P is a vulcanized NBR elastomer with the same quantity of DOS plasticizer as well as silica and carbon black fillers. Compound NBR-F-P simulates a commercial compound with a durometer Shore hardness of 68 A. The compound formulation NBR-F-nP is a vulcanized NBR elastomer with carbon black and silica fillers but no plasticizer. The materials were supplied in 15 cm × 15 cm × 0.3 cm plaques.

Table 1. NBR compounds composition.

Composition (parts per hundred NBR)	NBR-nF-nP	NBR-nF-P	NBR-F-P	NBR-F-nP
NBR (Nipol 1042)	100	100	100	100
Stearic acid	1	1	1	1
Zinc oxide	5	5	5	5
Sulfur	1.5	1.5	1.5	1.5
MBTS 2,2'-Benzothiazyl Disulfide	1.5	1.5	1.5	1.5
TMTD Bis(dimethylthiocarbamoyl) Disulfide	0.5	0.5	0.5	0.5
DOS		10	10	
Carbon black (n330)			23	19
Silica (Nipsil VN3)			28	23
Density	1.032	1.015	1.182	1.175
Hardness (Shore A Durometer)	51.0	43.4	65.8	68.7

2.2 Experimental test setup

The pressure vessel was purged with argon before any hydrogen tests were performed for safety reasons. High-pressure hydrogen exposure was conducted using 99.99% hydrogen gas with pressures up to 90 MPa in a pressure vessel. A 22.2 mm diameter disk with a thickness of 2.9 mm was cut from each of the vulcanized plaques. Depending on the experiment, samples were exposed to various pressures from 27.6–90 MPa at an approximate flow rate of 2.5 MPa/min. The system was held isostatic for 16 h to ensure that specimens were fully saturated with hydrogen and that the temperature reached equilibrium. A second filling was done to replenish the vessel to make up pressure lost due to the adiabatic cooling of the hydrogen gas during the initial filling. The high-pressure hydrogen gas was then released at a depressurization rate of more than 0.34 MPa/min. After the exposure experiment was complete, the vessel was flushed with argon to eliminate the remaining hydrogen for safety.

A high-pressure manifold system designed and built at Sandia National Laboratories was used to prep the hydrogen pressure cycled specimens. The specimens were initially soaked in 90MPa hydrogen at 55 °C for 36 hours, to ascertain complete saturation. Then, the pressure was decreased to 2 MPa over a duration of 0.1 hour, held at 2

MPa for a duration of 1 hour, and pumped back up to 90 MPa within 0.1 hour. This marks the end of one cycle. This process was repeated for 100 times in this study. After the last cycle, the system was completely pressure released and purged with inert gas before opening the vessel to retrieve the specimens.

2.3 Compression set

Compression set tests were conducted both before hydrogen exposure and 30 min after exposure at hydrogen gas pressures up to 90 MPa for 22 h at 110°C. The dimensions of the specimens were first measured using a laser micrometer before they were placed on the bottom plate of the compression setup previously described in the work of Menon et al. [30] A constant deflection of 25% was applied to the specimens, with a 2.35 mm thick space bar in accordance with the ASTM standard D395, Method B. Then, the dimensions were measured with the laser micrometer after removal from the compression setup and given a 30 min recovery at room temperature (~23 °C). Compression-set ratios were calculated as a percentage of the original deflection using the equation below:

$$C_B = \left[\frac{(t_0 - t_1)}{(t_0 - t_n)}\right] \times 100\% \quad (1)$$

where C_B stands for compression set in percentage, t_0 for original thickness of the specimen, t_1 for final thickness of the specimen, and t_n for thickness of the spacer bar.

2.4 Density tests

Density measurements were performed following the same method as used in the prior work of Menon et al. [30] Based on ASTM D792-13, the specimens were measured immediately after 90 MPa hydrogen exposure and 48 h after removal from the pressure vessel. Weights were determined in air using a Mettler Toledo XS403S balance with a repeatability of 0.5 mg ± 0.0008% gross weight of the specimen. The specimens were then immersed in deionized water using the designated setup and their apparent masses after immersion were determined. The water temperature, water density, and air density at 21°C were used to calculate density, using the following equation:

$$\boldsymbol{\rho} = \left[\frac{(\boldsymbol{W_{air}})}{(\boldsymbol{W_{air}} - \boldsymbol{W_{water}})}\right] \times (\boldsymbol{D_{water}} - \boldsymbol{D_{air}}) + \boldsymbol{D_{air}} \quad (\mathbf{2})$$

where $\boldsymbol{\rho}$ is the density of the specimen, $\boldsymbol{W_{air}}$ is the weight of the specimen in air at 21°C, $\boldsymbol{W_{water}}$ is the weight of the specimen in water at 21°C, $\boldsymbol{D_{water}}$ is the density of water at 21°C, and $\boldsymbol{D_{air}}$ is the density of air at 21°C.

2.5 Micro-computed tomography

Internal microstructural damage in the elastomers was characterized by micro-computed tomography (micro-CT). A Zeiss Xradia 520 Versa with a max resolution of 1 micron was used. Each sample was imaged at ~0.7 mm field of view and a pixel size of ~0.7 µm. Typical 2D images from the experiments are produced to examine the sate of the polymer after hydrogen exposure and to enable discerning voids, cracks and tother anomalies in the materials due to hydrogen diffusion.

2.6 Helium-ion microscopy

Image analyses of surfaces and through-thickness fractures were performed using a Zeiss ORION PLUS helium-ion microscope (HeIM). The HeIM has a resolution of less than 0.3 nm at an energy of 25–30 kV and beam currents between 1 fA and 25 pA. Depending on the substrate material, the helium-ion beam produces 3–9 secondary electrons for each incoming helium ion. This creates a better signal and higher image contrast between different materials that is not seen with a traditional scanning electron microscope.

2.7 Transmission electron microscopy

The material was dissected to 0.5 × 0.5 × 2 mm cuboids, mounted with 2.3% sucrose solution on specimen carriers (Leica Microsystems, #16701952), and flash-frozen in liquid nitrogen. Ultrathin sections (70 nm) were prepared using a Leica UC7 ultramicrotome operating at −120°C. They were collected on 100 mesh Cu grids coated with Formvar and carbon (Electron Microscopy Sciences) and imaged with a Tecnai T-12 TEM (FEI) operating at 120 kV with a LaB_6 filament. Images were collected digitally using a 2_2K UltraScan 1000 charge-coupled device camera (Gatan).

2.8 X-ray diffraction (XRD) analysis

The XRD patterns of model NBR sampls were obtained with a Rigaku desktop X-ray diffractometer using Cu Ka (1.54059 Å) radiation with the X-ray generator operatign at 20 kV and 30 mA. Data was collected for a 2θ range of 10-80 degrees at an angular resolution of 0.01 degree/s. Zinc oxide crystal sizes were calculated using the Scherer equation at 2θ = 20°, and peak characterization was performed using an XRD software (PDX2) library.

3.0 RESULTS AND DISCUSSION

Figure 1 shows both the effects of 90 MPa, high-pressure hydrogen at 110°C for 22 hours on the compression-set performance of the four NBR compounds and the changes that occurred before and after hydrogen pressure exposure. The results clearly indicate that the addition of plasticizer (i.e., DOS) caused the additional increase in compression set after hydrogen exposure, as NBR-nF-P and NBR-F-P showed a 65.8% increase and a 36.6% increase, respectively, while neither did NBR-nF-nP or NBR-F-nP change by more than 19%. Since our prior study [28] confirmed that plasticizer migrates and concentrates when subject to hydrogen exposure, we attributed such changes in compression set to a combinational effect of the hydrogen-provoked plasticizer migration and the hydrogen dissolved within polymer. After 100 pressure cycles, all compounds were found to have modest decrease in compression set values. This is likely due to the hydrogen degradation effects that could break down the polymer chains and cumulatively created numerous micro-voids throughout multiple rapid decompression processes. Both filled compunds (i.e., NBR-F-P and NBR-F-nP) presented a ≤10% average drop while slightly more reduction (27% for NBR-nF-nP and 13% for NBR-nF-P) in compression set values was posted for unfilled systems after the pressure cycling experiments. Such different behavior was ascribed to the fact that the fillers can reinforce the matrix polymer and mitigate crack initiation to some extent.

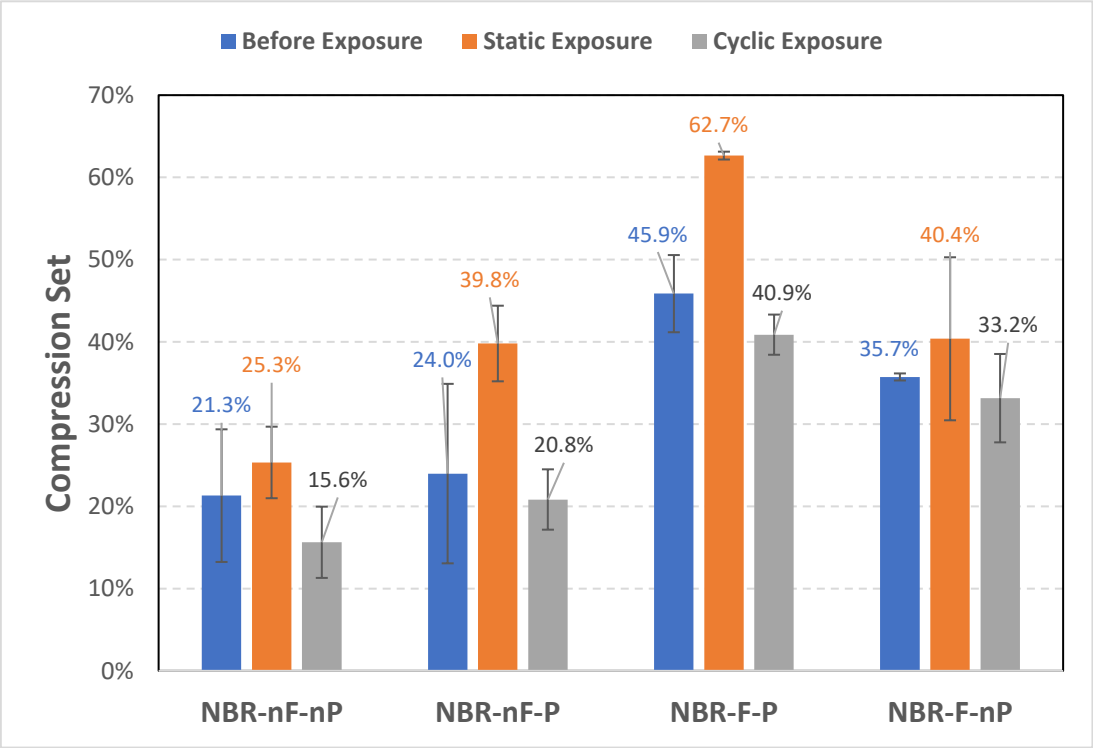

Figure 1. Effects of high-pressure hydrogen exposure on compression set.

Density changes are usually used to indicate the sorption properties of gases when transported through polymers, and porosity and internal material damage. We found a noticeable decrease (>35%) in density for all model NBRs immediately after exposure. This phenomenon is primarily attributed to the volume increase caused by the limited diffusion rate of hydrogen within the polymer upon removal of the external pressure. Then, all samples regained the density lost in 48 hours after hydrogen exposure, which suggests that the hydrogen trapped in the polymer had escaped almost completely. However, we observed up to a 30% permanent decrease in density across all compounds after the 100 pressure cycles of hydrogen exposure, indicative of significant volumetric expansion which lends strong support to our earlier interpretation on the compression set percentage losses and internal material damage.

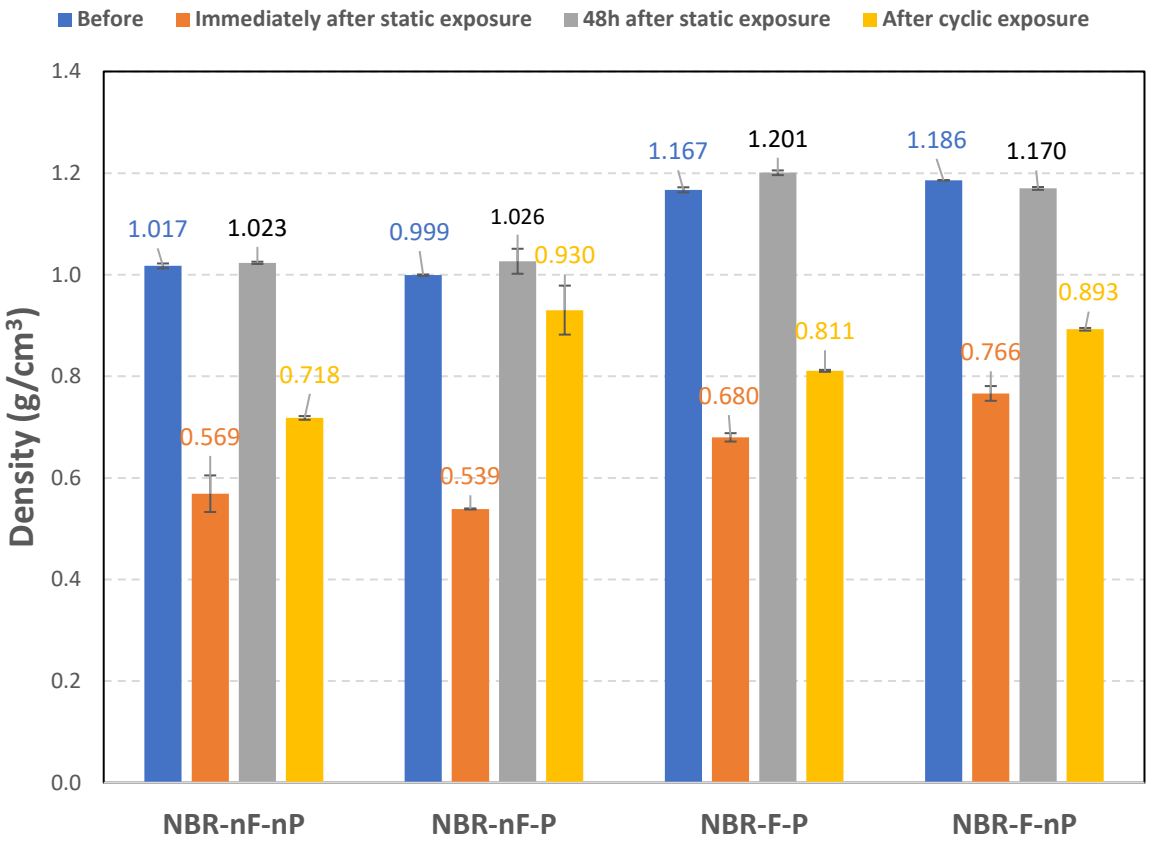

Figure 2. Effects of high-pressure hydrogen exposure on density.

Figure 3 shows the internal material morphology with micro-CT of all four model compounds at the micrometer level after exposure to 90 MPa hydrogen gas. In particular, the damage formed in the unfilled, unplascitized system (NBR-nF-nP) post-exposure mostly take the form of slits and cracks with a small fraction being round voids. When there is plasticizer added to the rubber (both NBR-nF-P and NBR-F-P), round voids became the predominant form of damage with a significanly increased quantity. We postulated that the added plasticizer results in lower density and more space for hydrogen to concentrate given different solubility of hydrogen in plastizier from in polymer, which is evidenced by more density losses seen in plasticized compounds than in unplasticized counterparts immediately after static exposure. For NBR-F-nP, the presence of fillers and lack of plasticizer resulted in much fewer voids through static exposure to high pressure hydrogen gas. In addition, the voids formed were generally small-to-medium sized. We concluded that the damage mitigation by fillers is quite effective at the micrometer scale while plasticizer significantly undermines it when present

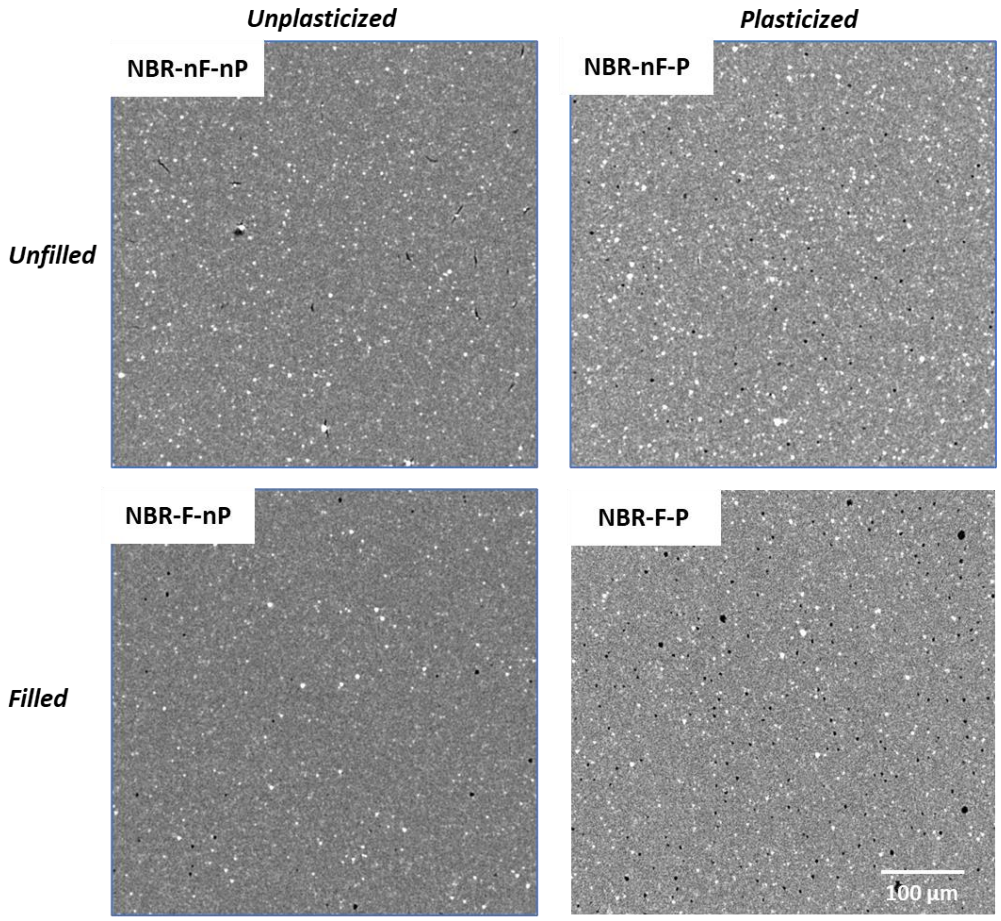

Figure 3. Micro-CT images of model NBR samples after static exposure to 90 MPa hydrogen. The white particles are zinc oxide and black regions are pores or cracks. Scale bar = 100 µm.

Along this line, HeIM was utilized to visually inspect the surface morphology of model NBRs before and after hydrogen treatment at the next level down. HeIM is an advanced, unqiue imaging tool at PNNL, which is capable of forming a more tightly focused beam to provide a up to 4 times better image resolution than conventional scanning electron microscopy (SEM) due to the shorter wavelength of helium ion. Another advantage associates HeIM proceducing 3-9 secondary electrons for each incoming heliun ion over SEM typically creating just one secondary electron for each incoming electron, which enables a better signal with higher contrast between different materials. Figure 4 is composed of images at the surface of each material as-received, after static exposure to 28 MPa hydrogen, and after cyclic exposure to 90 MPa hydrogen, respectively. Neither of unplasticized rubber compounds (i.e., NBR-nF-nP and NBR-F-nP) showed noticeable morphological alteration at this small length scale after static exposure or cyclic exposure. However, NBR-nF-P and NBR-F-P experienced a heavy migration of the DOS plasticizer by forming dark spots in the statically exposed samples or

large dark regions in the cyclically exposed samples. This observation aligns well with the micro-CT results, indicating the hydrogen effects on material morphology and consequentially damage formation.

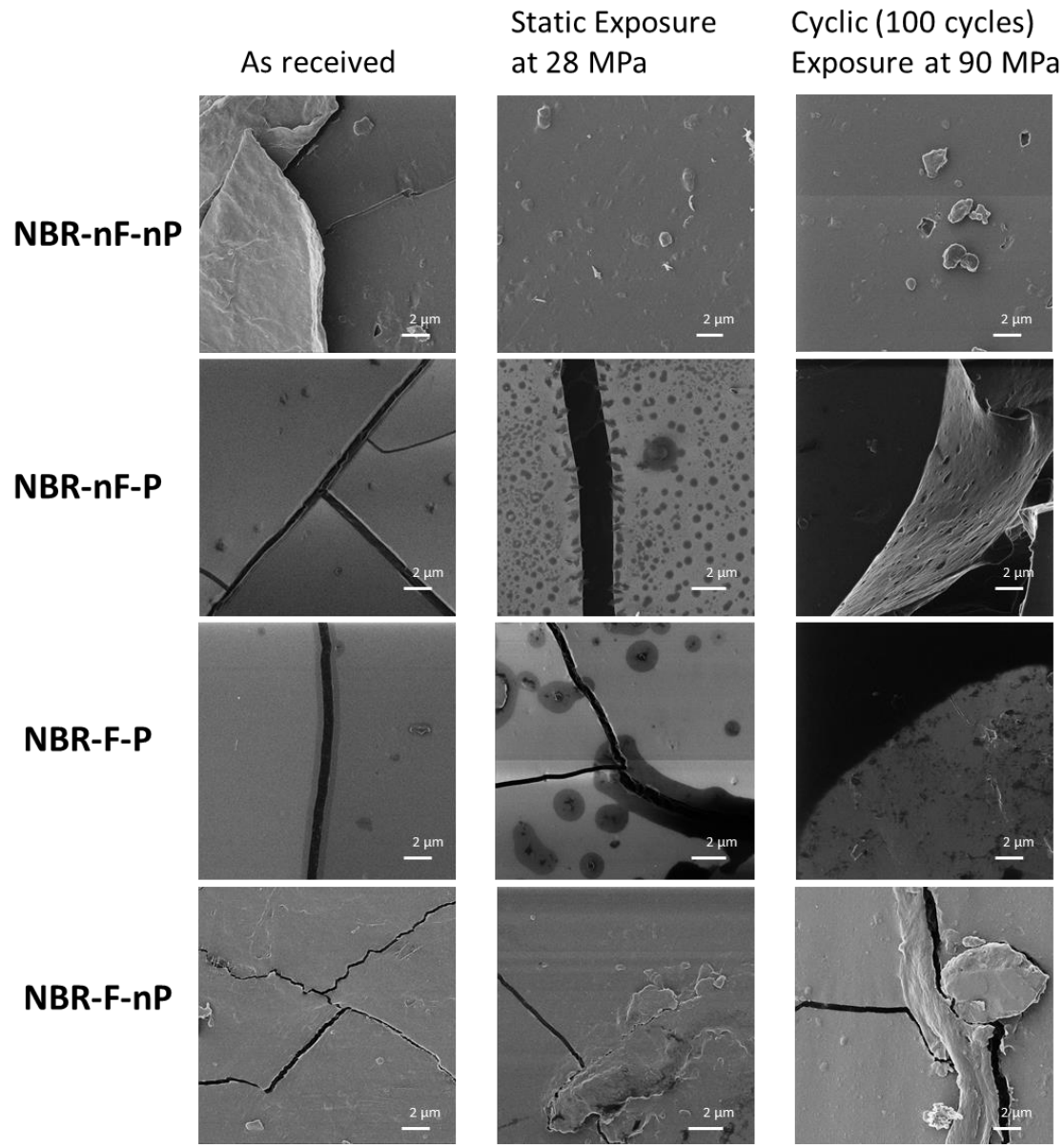

Figure 4. HeIM images for surface of model NBR samples as received (unexposed), after static exposure to 28 MPa hydrogen, and after cyclic exposure to 90 MPa hydrogen.

Microtome has been widely used in the science community as a advanced cutting tool for preparation of extremely thin slices of material for observation under transmitted light or electron radiation. NBR-nF-P and NBR-F-P were sectioned into slices about 70 nm thick which were subsequently mounted on copper grids for imaging. Figure 5 shows the change in internal morphology of these two rubber compounds before and after static exposure to 28 MPa hydrogen gas. Interestingly, gray “halo” structure was found appearing around the zinc oxide particles (dark particles shown in the images) in NBR-nF-P after hydrogen exposure. This could be evidence of interfacial detachment between zinc oxide particles and polymer matrix caused by hydrogen. Additionally, there were more smaller zinc oxide particles (<30 nm) in the exposed sample than in the as-received sample. In contrast, we observed that smaller filler particles of carbon black and silica in NBR-F-P become less uniformly distributed after exposure to hydrogen, leaving many filler-lacking regions (the far right column in Figure 5). We speculate that it relates, if not all, to filler particle migration in these extreme conditions, and this could affect hydrogen diffusion behavior.

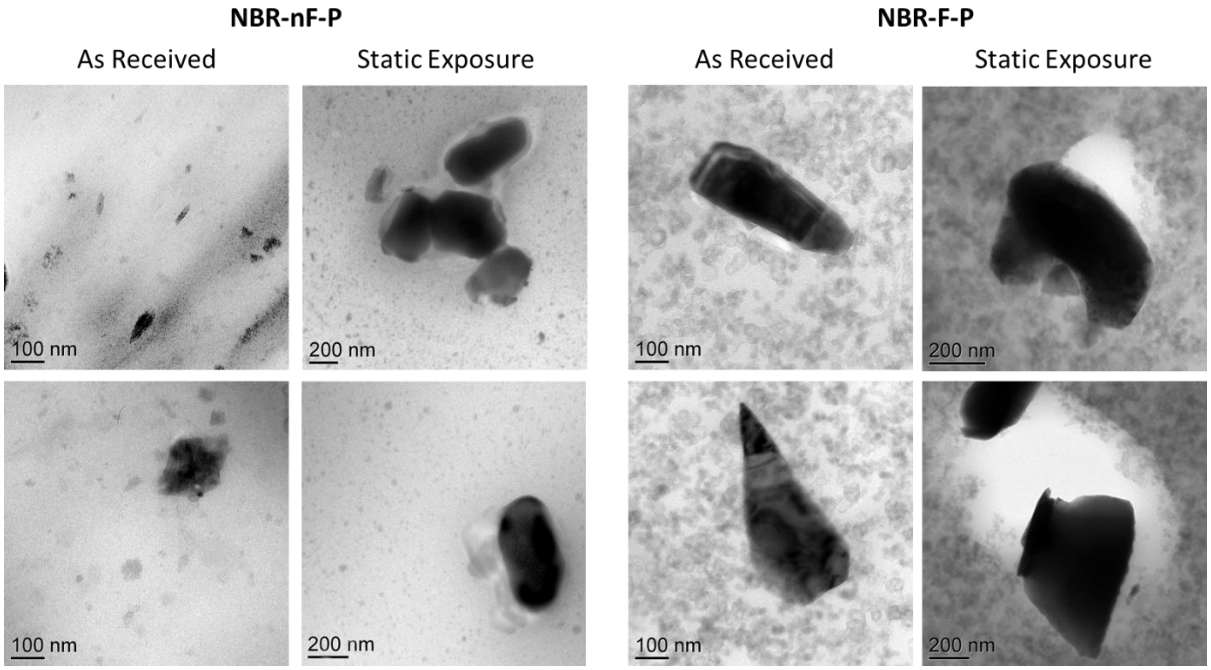

Figure 5. TEM images for NBR-nF-P and NBR-F-P: as received and after static exposure at 28 MPa.

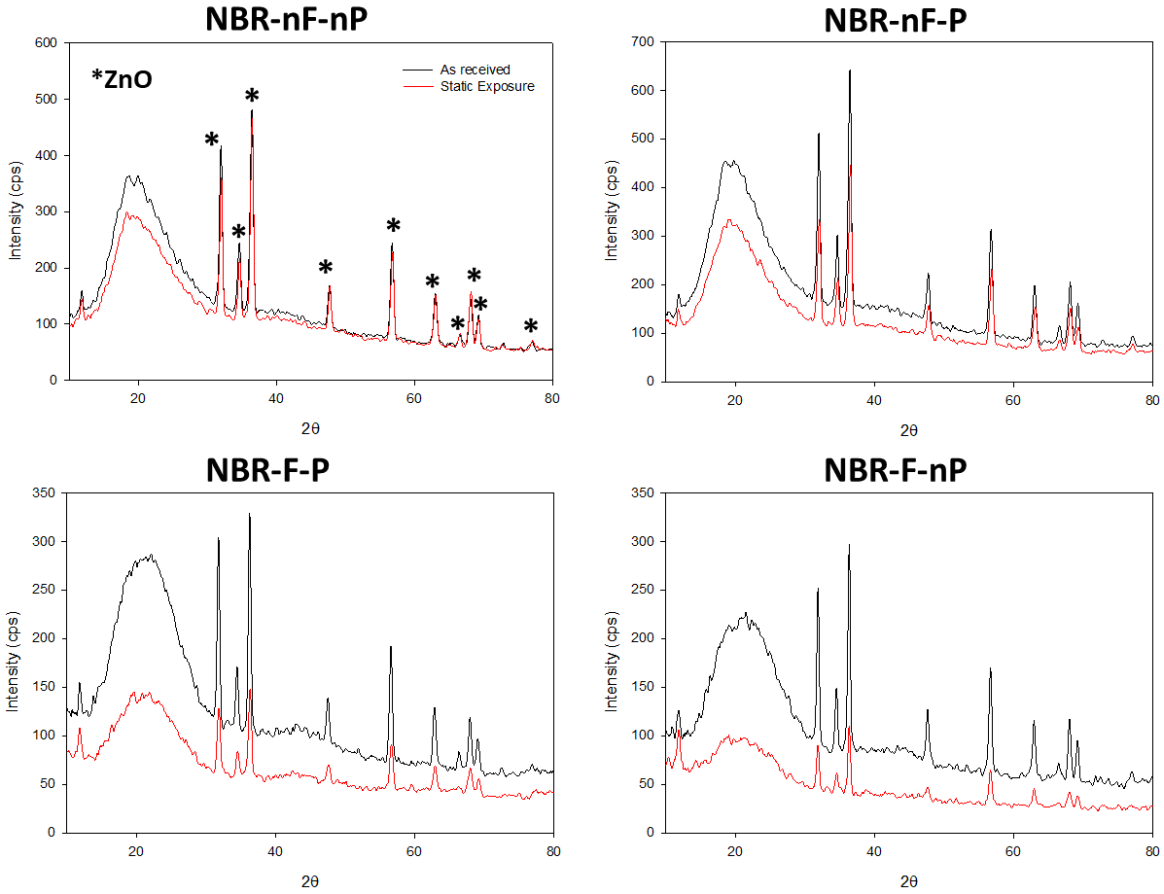

Figure 6. XRD profiles for model NBR compounds (black line: as received; red line: after static exposure at 28 MPa)

X-ray diffraction (XRD) is a non-destructive test method used to identify the crystalline phases present in a material and thereby reveal chemical composition information. Zinc oxide typically exists in the form of crystals,

so XRD can be used to study any structural change to zinc oxide and surrounding matrix material as TEM suggested significant alteration in morphology around zinc oxide after hydrogen exposure. Figure 6 shows XRD patterns for all four NBR compounds and we observed no major change in chemical structure as the patterns are identical before and after hydrogen exposure. The Bragg's law was used to estimate the crystal size of zinc oxide particles and the results are summarized in Table 2. The zinc oxide particle decreased in size, after exposure to 28 MPa hydrogen, for all model compounds except NBR-nF-nP. This agrees with our TEM observations where the quantity of smaller zinc oxide particles increased after the hydrogen treatment.

Table *2*. XRD data analysis.

	ZnO size (nm)	d spacing (Å) at 2θ ~20
NBR-nF-nP (as received)	**19.9**	**4.611**
NBR-nF-nP (static exposure)	**34.8**	**4.604**
NBR-nF-P (as received)	**30**	**4.637**
NBR-nF-P (static exposure)	**21.7**	**4.604**
NBR-F-P (as received)	**35.1**	**4.203**
NBR-F-P (static exposure)	**22.6**	**4.137**
NBR-F-nP (as received)	**38**	**4.205**
NBR-F-nP (static exposure)	**30.7**	**4.275**

4.0 CONCLUSIONS

With increasing utilization of hydrogen as a promising energy alternative to fossil fuel, constrcution of the hydrogen infrastructure and manufacture of hydrogen fuel cell vehicles have raisen the performance requirement for polymer materials with both static and dynamic sealing as well as high barrier properties. It is therefore of high importance to understand why each polymer system behaves differently on a submicron scale, which is less explored. Improved understanding will benefit design and development of new material formuations with a higher resistance to hydrogen degradation.

The present work was focused on a series of model NBR compounds which differ from each other by incorporation of DOS plasticizer and/or carbon black and silica filler. Hydrogen has a profound effect on the DOS plasticizer and thereby its migration resulting in mophological changes. Carbon black and silica fillers are very effective on mitigating damages like voids and cracks when subject to high pressure hydrogen. Advanced imaging techniques were used to reveal the hydrogen effects at different length scales on the morphology of the material and plays an important role in helping us understand the origin of damages. Our observation suggested that the plasticizer migration and the zinc oxide particles have shown the most significant alteration during hydrogen exposure. Future work needs to explore the hydrogen effects with a large number of cycles in order to provide better understanding for polymer materials performance in the end-use conditions.

ACKNOWLEDGEMENTS

This work was fully supported by the U.S. Department of Energy (USDOE), Office of Energy Efficiency and Renewable Energy (EERE), Hydrogen and Fuel Cells Technologies Office (HFTO) under Contract Number DE-AC05-76RL01830. We aslo knowledge support from the Environmental Molecular Sciences Larboratory (EMSL). EMSL is a ntional scientific user facitility sponsored by the DOE's Office of Science, Biological and Environmental Research program that is located at Pacific Northwest National Laboraoty. We also thankfully acknowledge Bernice Mills , Sandia National Laboratories, for her important contributions to this work through the USDOE Hydrogen Materials Compatibility program, H-Mat. Sandia National Laboratories is a multimission laboratory managed and operated by National Technology & Engineering Solutions of Sandia, LLC, a wholly owned subsidiary of Honeywell International Inc., for the U.S. Department of Energy's National Nuclear Security Administration under contract DE-NA0003525.

DISCLAIMER

The views and opinions of the authors expressed herein do not necessarily state or reflect those of the United States Government or any agency thereof. Neither the United States Government nor any agency thereof, nor any of their employees, makes any warranty, expressed or implied, or assumes any legal liability or responsibility for the accuracy, completeness, or usefulness of any information, apparatus, product, or process disclosed, or represents that its use would not infringe privately owned rights.

This paper describes objectives technical results and analysis. Any subjective views or opinions that might be expressed in the paper do not necessarily represent the views of the U.S. Department of Energy or the United States Government.

REFERENCES

1. Schlapbach, L. and Züttel, A., Hydrogen-Storage Materials for Mobile Applications, *Nature*, **414**, 2002, pp. 353-358.
2. Eberle, U., Müller, B., and von Helmolt, R., Fuel Cell Electric Vehicles and Hydrogen Infrastructure: Status 2012, *Energy & Environmental Science*, **5**, 2012, pp. 8780-8798.
3. Jain, I. P., Hydrogen the Fuel for 21st Century, *International Journal of Hydrogen Energy*, **34**, 2009, pp. 7368-7378.
4. Schlapbach, L., Hydrogen-Fueled Vehicles, *Nature*, **460**, 2009, pp. 809-811.
5. Woodtli, J. and Kieselbach, R., Damage Due to Hydrogen Embrittlement and Stress Corrosion Cracking, *Engineering Failure Analysis*, **7**, No. 6, 2000, pp. 427-450.
6. Djukic, M. B., Sijacki Zeravcic, V., Bakic, G. M., Sedmak, A., and Ragjicic, B., Hydrogen Damage of Steels: A Case Study and Hydrogen Embrittlement Model, *Engineering Failure Analysis*, **58**, pt.2, 2015, pp. 485-498.
7. Alvine, K. J., Shutthanandan, V., Arey, B. W., Wang, C., Bennett, W. D., and Pitman, S. G., Pb Nanowire Formation on Al/Lead Zirconate Titanate Surfaces in High-Pressure Hydrogen, *Journal of Applied Physics*, **112**, 2012, 013533.
8. Madina, V., Azkarate, I., Compatibility of Materials with Hydrogen. Particular Case: Hydrogen Embrittlement of Titanium Alloys, *Internation Journal of Hydrogen Energy*, **34**, 2009, pp. 5976-5980.
9. Jaravel, J., Castagnet, S., Grandidier, J., and Benoit, G., On Key Parameters Influencing Cavitation Damage upon Fast Decompression in a Hydrogen Saturated Elastomer, *Polymer Testing*, **30**, No. 8, 2011, pp. 811-818.
10. Schrittesser, B., Pinter, G., Schwarz, Th., Kadar, Z., and Nagy, T., Rapid Gas Decompression Performance of Elastomers – A Study of Influencing Testing Parameters, *Procedia Structural Integrity*, **2**, 2016, pp. 1746-1754.
11. Yamabe, J., Nishimura, S., Influence of Fillers on Hydrogen Penetration Properties and Blister Fracture of Rubber Composites for O-Ring Exposed to High-Pressure Hydrogen Gas, *International Journal of Hydrogen Energy*, **34**, 2009, pp. 1977-1989.
12. Yamabe, J., Nishimura, S., Koga, A., A Study on Sealing Behavior of Rubber O-Ring in High Pressure Hydrogen Gas, *SAE International Journal of Materials and Manufacturing*, **2**, 2009, pp. 452-460.
13. Yamabe, J., Fujiwara, H., Nishimura, S., Fracture Analysis of Rubber Sealing Material for High Pressure Hydrogen Vessel, *Nihon Kikai Gakkai Ronbunshu, A Hen/Transactions of the Japan Society of Mechanical Engineers, Part A*, **75**, 2009, pp. 1063-1073.
14. Yamabe, J., Matsumoto, T., Nishimura, S., Application of Acoustic Emission Method to Detection of Internal Fracture of Sealing Rubber Material by High-Pressure Hydrogen Decompression, *Polymer Testing*, **30**, 2011, pp. 76-85.
15. Yamabe, J., Nishimura, S., Nanoscale Fracture Analysis by Atomic Force Microscopy of EPDM Rubber Due to High-Pressure Hydrogen Decompression, *Journal of Materials Science*, **46**, 2011, pp. 2300-2307.
16. Fujiwara, H., Nishimura, S., Evaluation of Hydrogen Dissolved in Rubber Materials under High-Pressure Exposure Using Nuclear Magnetic Resonance, *Polymer Journal*, **44**, 2012, pp 832-837.

17. Nishimura, S., Fujiwara, H., Detection of Hydrogen Dissolved in Acrylonitrile Butadiene Rubber by ^{1}H Nuclear Magnetic Resonance, *Chemical Physics Letters*, **522**, 2012, pp. 43-45.

18. Fujiware, H., Yamabe, J., Nishimura, S., Evaluation of the Change in Chemical Structure of Acrylonitrile Butadiene Rubber after High-Pressure Hydrogen Exposure, *International Journal of Hydrogen Energy*, **37**, 2012, pp. 8729-9733.

19. Koga, A., Uchida, K., Yamabe, J. Nishimura, S., Evaluation on High-Pressure Hydrogen Decompression Failure of Rubber O-ring Using Design of Experiments, *International Journal of Automotive Engineering*, **2**, 2011, pp. 123-129.

20. Yamabe, J., Nishimura, S., Tensile Properties and Swelling Behavior of Sealing Rubber Materials Exposed to High-Pressure Hydrogen Gas, *Journal of Solid Mechanics and Materials Engineering*, **6**, 2012, pp. 466-477.

21. Yamabe, J., Koga, A., Nishimura, S., Failure Behavior of Rubber O-Ring under Cyclic Exposure to High-Pressure Hydrogen gas, *Engineering Failure Analysis*, **35**, 2013, pp. 193-205.

22. Fujiware, H., Ono, H., Nishimura, S., Degradation Behavior of Acrylonitrile Butadiene Rubber after Cyclic High-Pressure Hydrogen Exposure, *International Journal of Hydrogen Energy*, **40**, 2015, pp. 2025-2034.

23. Ohyama, K., Fujiware, H., Nishimura, S., Inhomogeneity in Acrylonitrile Butadiene Rubber during Hydrogen Elimination Investigated by Small-Angle X-ray Scattering, *International Journal of Hydrogen Energy*, **43**, 2018, pp. 1012-1024.

24. Castagnet, S., Mellier, D., Nait-Ali, A., Benoit, G., In-situ X-ray Computed Tomography of Decompression Failure in A Rubber Exposed to high-pressure gas, *Polymer Testing*, **70**, 2018, pp. 255-262.

25. Jung, J. K., Jeon, S. K., Kim, K., Lee, C. H., Baek, U. B., Chung, K. S., Impedance Spectroscopy for In Situ and Real-Time Observations of the Effects of Hydrogen on Nitrile Butadiene Rubber Polymer under High Pressure, *Scientific Reports*, **9**, 2019, pp. 13035.

26. Kim, K., Jeon, H., Kang, Y., Kim, W., Yeom, J., Chio, S., Cho, S., Behaviour of EPDM Rubber for Fuel Cell Vehicle Application under High-Pressure Hydrogen Evironment, *Transcations of the Korean Hydrogen and New Energy Society*, **31**, 2020, pp. 453-458.

27. Jung, J. K., Kim, I. G., Kim, K. T., Ryu, K. S., Chung, K. S., Evaluation Techniques of Hydrogen Permeation in Sealing Rubber Materials, *Polymer Testing*, **93**, 2021, pp. 107016.

28. Simmons, K. L., Kuang, W., Burton, S. D., Arey, B. W., Shin, Y., Menon, N. C., Smith, D. B., H-Mat Hydrogen Compatibility of Polymers and Elastomers, International Journal of Hydrogen Energy, https://doi.org/10.1016/j.ijhydene.2020.06.218.

29. Kuang, W., Bennett, W. D., Roosendaal, T. J., Arey, B. W., Dohnalkova, A., Petrossian, G., Simmons, K. L., In Situ Friction and Wear Behavior of Rubber Materials Incorporating Various Fillers and/or A Plasticier in High-Pressure Hydrogen, *Tribology International*, **153**, 2021, pp. 106627.

30. Menon, N. C., Kruizenga, A. M., Alvine, K. J., San Marchi, C., Nissen, A., Behaviour of Polymers in High Pressure Environments as Applicable to the Hydrogen Infrastructure, Proceedings of the ASME 2016 Pressure Vessels and Piping Conference, 17-21 July 2016, Vancouver, BC, Canada.

31. Walter, E.D., Qi, L., Chamas, A., Mehta, H.S., Sears, J.A., Scott, S.L., Hoyt, D.W., *Operando* MAS-NMR Reaction Studies at High Temperatures and Pressures, *J. Phys. Chem. C*, **122**, No. 15, 2018, pp. 8209-8215.

32. Lawandy, S. N., Halim, S. F., Darwish, N. A., Structure Aggregation of Carbon Black in Ethylene-Propylene Diene Polymer, *eXPRESS Polymer Letters*, **3**, No. 3, 2009, 152-158.

33. Nishimura, S., Polymeric Materials for Hydrogen Devices, International Symposium of Hydrogen Polymers Team, Hydrogenius, 2 February 2018, Kyushu University, Japan.